

Non-Abelian dual Meissner effect in SU(3) Yang-Mills theory and confinement/deconfinement phase transition at finite temperature

Akihiro Shibata*

Computing Research Center, High Energy Accelerator Research Organization (KEK) & Graduate University for Advanced Studies (Sokendai), Tsukuba 305-0801, Japan
E-mail: akihiro.shibata@kek.jp

Kei-Ichi Kondo

Department of Physics, Graduate School of Science, Chiba University, Chiba 263-8522, Japan
E-mail: kondok@faculty.chiba-u.jp

Seikou Kato

Fukui National College of Technology, Sabae, Fukui 916-8507, Japan
E-mail: skato@fukui-nct.ac.jp

Toru Shinohara

Department of Physics, Graduate School of Science, Chiba University, Chiba 263-8522, Japan
E-mail: shinohara@graduate.chiba-u.jp

The dual superconductivity is a promising mechanism for quark confinement. We have proposed the non-Abelian dual superconductivity picture for SU(3) Yang-Mills theory, and showed the restricted field dominance (called conventionally Abelian dominance), and non-Abelian magnetic monopole dominance in the string tension. We have further demonstrated by measuring the chromoelectric flux that the non-Abelian dual Meissner effect exists and determined that the dual superconductivity for SU(3) case is of type I, which is in sharp contrast to the SU(2) case: the border of type I and type II.

In this talk, we focus on the confinement/deconfinement phase transition and the non-Abelian dual superconductivity at a finite temperature: We measure the Polyakov loop average and correlator and investigate the restricted field dominance in the Polyakov loop. Then, we measure the chromoelectric flux between a pair of static quark and antiquark created by a pair of Polyakov loops, and investigate the non-Abelian dual Meissner effect and its relevance to the phase transition.

From quarks and gluons to hadronic matter: A bridge too far ?

2-6 September, 2013

European Centre for Theoretical Studies in Nuclear Physics and Related Areas (ECT), Villazzano, Trento (Italy)*

*Speaker.

1. Introduction

The confinement problem is one of the most challenging problems in quantum chromodynamics (QCD). It has long been argued that the dual superconductivity is the promising mechanism for quark confinement [1]. In this scenario, the monopole condensation could play the dominant role for quark confinement. Quark confinement follows from the area law of the Wilson loop average, i.e., the string tension for quark and antiquark static potential must be observed. In many preceding works, the Abelian projection [2] was used to show the dual Meissner effect and to perform numerical analyses, which exhibited the remarkable results: Abelian dominance [3], magnetic monopole dominance [4], and center vortex dominance [5] in the string tension. However, these results are obtained only in special gauges: the maximal Abelian (MA) gauge and the Laplacian Abelian gauge within the Abelian projection, which breaks the gauge symmetry as well as color symmetry (global symmetry).

In order to overcome the shortcomings of the Abelian projection and establish the gauge independent (invariant) mechanism, for quark confinement we have proposed a new lattice formulation of $SU(N)$ Yang-Mills (YM) theory in the previous papers [6, 7] (as a lattice version of the continuum formulations [8, 9] for $SU(2)$ and [10, 11, 12] for $SU(N)$), which gives a decomposition of the gauge link variable suited for extracting the dominant modes for quark confinement in the gauge independent way. In the case of $SU(2)$, the decomposition of the gauge link variable was given on a lattice [13, 14, 15, 18] as a lattice version of the Cho-Duan-Ge-Faddeev-Niemi-Shabanov (CDGFNS) decomposition [8]. For the gauge group $G = SU(N)$ ($N \geq 3$), it was found [12] that the extension of the decomposition from $SU(2)$ to $SU(N)$ ($N \geq 3$) is not unique and that there are a number of possible ways of decompositions discriminated by the stability subgroup \tilde{H} of G , while there is the unique option of $\tilde{H} = U(1)$ in the $SU(2)$ case.

For the case of $G = SU(3)$, in particular, there are two possibilities which we call the maximal option and the minimal option [12]. The maximal option is obtained for the stability group $\tilde{H} = U(1) \times U(1)$, which enables us to give a gauge invariant version of the MA gauge as the Abelian projection [16, 29]. The minimal one is obtained for the stability group $\tilde{H} = U(2) \cong SU(2) \times U(1)$, which is suited for representing the Wilson loop in the fundamental representation as derived from the non-Abelian Stokes theorem [24, 25, 26]. In the static potential for a pair of quark and antiquark in the fundamental representation, we have demonstrated in [17, 19, 20] and [30]: (i) the restricted-field dominance or “Abelian” dominance (which is a gauge-independent (invariant) extension of the conventionally called Abelian dominance): the string tension σ_V obtained from the decomposed V -field (i.e., restricted field) reproduced the string tension σ_{full} of the original YM field, $\sigma_V/\sigma_{\text{full}} = 93 \pm 16\%$, (ii) the gauge-independent non-Abelian magnetic monopole dominance: the string tension σ_V extracted from the restricted field was reproduced by only the (non-Abelian) magnetic monopole part σ_{mon} , $\sigma_{\text{mon}}/\sigma_V = 94 \pm 9\%$.

To establish the non-Abelian dual superconductivity for quark confinement in $SU(3)$ YM theory which is claimed in [30], we must show the evidence of the dual Meissner effect by applying our new formulation to the $SU(3)$ YM theory on a lattice. In the first half of this talk, we give a brief review of [23]: First, we study the dual Meissner effect by measuring the distribution of chromo-flux created by a pair of static quark and antiquark. We compare the chromo-flux of the original YM field with that of the restricted field and examine if the restricted field corresponding to the stability group $\tilde{H} = U(2)$ reproduces the dual Meissner effect, namely, the dominant part of the chromoelectric field strength of $SU(3)$ YM theory. Second, we show the possible magnetic monopole current induced around the flux connecting a pair of static quark and antiquark. Third, we focus on the type of dual superconductivity, i.e., type I or type II. In the $SU(2)$ case, the extracted field corresponding to the stability group $\tilde{H} = U(1)$ reproduces the dual Meissner effect, which gives a gauge invariant version of MA gauge in the Abelian projection. We have shown that the dual

superconductivity of the $SU(3)$ YM theory is indeed the type I, in sharp contrast to the $SU(2)$ case: the border of type I and type II.

In the latter half of this talk, we study the confinement/deconfinement phase transition at finite temperature in view of the non-Abelian dual Meissner effect. We first study our new formulation of lattice YM theory at finite temperature: by using the decomposed V-field and original YM field, we measure the space average of Polyakov loops for each configuration, a Polyakov loop average and correlation functions of the Polyakov loops, and investigate whether the restricted field (V-field) plays the dominant role at finite temperature. Then, we measure the distribution of chromo-flux created by a pair of static quark and antiquark at finite temperature by using both the restricted field and the original YM field, and examine the chromo-electric flux tube is generated or not. We find disappearance of the dual Meissner effect (broken flux tube) at high temperature. Finally, we give summary and outlook

2. Method

2.1 Gauge Link Decomposition

We introduce a new formulation of the lattice YM theory of the minimal option, which extracts the dominant mode of the quark confinement for $SU(3)$ YM theory[30, 20], since we consider the quark confinement in the fundamental representation. Let $U_{x,\mu} = X_{x,\mu}V_{x,\mu}$ be the decomposition of YM link variable, where $V_{x,\mu}$ could be the dominant mode for quark confinement, and $X_{x,\mu}$ the remainder part. The YM field and the decomposed new-variables are transformed by full $SU(3)$ gauge transformation Ω_x such that $V_{x,\mu}$ is transformed as the gauge link variable and $X_{x,\mu}$ as the site available:

$$U_{x,\mu} \longrightarrow U'_{x,\mu} = \Omega_x U_{x,\mu} \Omega_{x+\mu}^\dagger, \quad (2.1a)$$

$$V_{x,\mu} \longrightarrow V'_{x,\mu} = \Omega_x V_{x,\mu} \Omega_{x+\mu}^\dagger, \quad X_{x,\mu} \longrightarrow X'_{x,\mu} = \Omega_x X_{x,\mu} \Omega_x^\dagger. \quad (2.1b)$$

The decomposition is given by solving the defining equation:

$$D_\mu^\varepsilon[V]\mathbf{h}_x := \frac{1}{\varepsilon} [V_{x,\mu}\mathbf{h}_{x+\mu} - \mathbf{h}_x V_{x,\mu}] = 0, \quad (2.2a)$$

$$g_x := e^{i2\pi q/3} \exp(-ia_x^0 \mathbf{h}_x - i \sum_{j=1}^3 a_x^{(j)} \mathbf{u}_x^{(i)}) = 1, \quad (2.2b)$$

where \mathbf{h}_x is an introduced color field $\mathbf{h}_x = \xi(\lambda^8/2)\xi^\dagger \in [SU(3)/U(2)]$ with λ^8 being the Gell-Mann matrix and ξ the $SU(3)$ gauge element. The variable g_x is undetermined parameter from Eq.(2.2a), $\mathbf{u}_x^{(j)}$'s are $su(2)$ -Lie algebra values, and q_x an integer value 0, 1, 2. These defining equations can be solved exactly [7], and the solution is given by

$$X_{x,\mu} = \widehat{L}_{x,\mu}^\dagger \det(\widehat{L}_{x,\mu})^{1/3} g_x^{-1}, \quad V_{x,\mu} = X_{x,\mu}^\dagger U_{x,\mu} = g_x \widehat{L}_{x,\mu} U_{x,\mu}, \quad (2.3a)$$

$$\widehat{L}_{x,\mu} = (L_{x,\mu} L_{x,\mu}^\dagger)^{-1/2} L_{x,\mu}, \quad (2.3b)$$

$$L_{x,\mu} = \frac{5}{3} \mathbf{1} + \frac{2}{\sqrt{3}} (\mathbf{h}_x + U_{x,\mu} \mathbf{h}_{x+\mu} U_{x,\mu}^\dagger) + 8 \mathbf{h}_x U_{x,\mu} \mathbf{h}_{x+\mu} U_{x,\mu}^\dagger. \quad (2.3c)$$

Note that the above defining equations correspond to the continuum version: $D_\mu[\mathcal{V}]\mathbf{h}(x) = 0$ and $\text{tr}(\mathbf{h}(x)\mathcal{X}_\mu(x)) = 0$, respectively. In the naive continuum limit, we have the corresponding decomposition $\mathbf{A}_\mu(x) = \mathbf{V}_\mu(x) + \mathbf{X}_\mu(x)$ in the continuum theory [12] as

$$\mathbf{V}_\mu(x) = \mathbf{A}_\mu(x) - \frac{4}{3} [\mathbf{h}(x), [\mathbf{h}(x), \mathbf{A}_\mu(x)]] - ig^{-1} \frac{4}{3} [\partial_\mu \mathbf{h}(x), \mathbf{h}(x)], \quad (2.4a)$$

$$\mathbf{X}_\mu(x) = \frac{4}{3} [\mathbf{h}(x), [\mathbf{h}(x), \mathbf{A}_\mu(x)]] + ig^{-1} \frac{4}{3} [\partial_\mu \mathbf{h}(x), \mathbf{h}(x)]. \quad (2.4b)$$

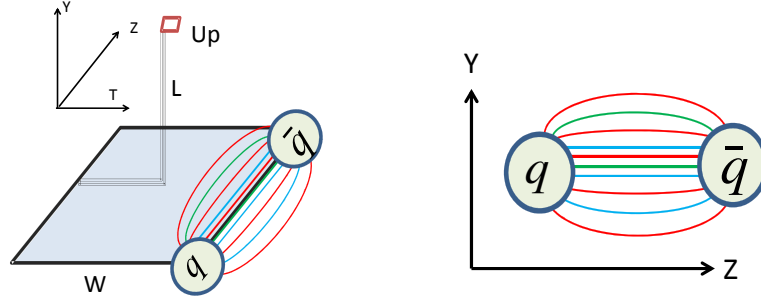


Figure 1: (Left) The connected correlator $\langle U_p L W L^\dagger \rangle$ between a plaquette U_p and the Wilson loop W . (Right) Measurement of the chromo flux in the Y-Z plane.

The decomposition is uniquely obtained as the solution of Eqs.(2.3), if color fields $\{\mathbf{h}_x\}$ are obtained. To determine the configuration of color fields, we use the reduction condition which makes the theory written by new variables $(X_{x,\mu}, V_{x,\mu})$ equipollent to the original YM theory. Here, we use the reduction function

$$F_{\text{red}}[\mathbf{h}_x] = \sum_{x,\mu} \text{tr} \{ (D_\mu^\varepsilon[U_{x,\mu}]\mathbf{h}_x)^\dagger (D_\mu^\varepsilon[U_{x,\mu}]\mathbf{h}_x) \}, \quad (2.5)$$

and color fields $\{\mathbf{h}_x\}$ are obtained by minimizing the functional.

2.2 Chromo-flux created by a pair of quark and antiquark

We investigate the non-Abelian dual Meissner effect as the mechanism of quark confinement. In order to extract the chromo-field, we use a gauge-invariant correlation function proposed in [27]: The gauge-invariant chromo-field strength $F_{\mu\nu}[U]$ created by a quark-antiquark pair in $SU(3)$ YM theory is measured by using a gauge-invariant connected correlator between a plaquette and the Wilson loop (see Fig.1):

$$F_{\mu\nu}[U] := \varepsilon^{-2} \sqrt{\frac{\beta}{6}} \rho_W[U], \quad \rho_W[U] := \frac{\langle \text{tr}(U_P L[U]^\dagger W[U] L[U]) \rangle}{\langle \text{tr}(W[U]) \rangle} - \frac{1}{3} \frac{\langle \text{tr}(U_P) \text{tr}(W[U]) \rangle}{\langle \text{tr}(W[U]) \rangle}, \quad (2.6)$$

where $\beta := 6/g^2$ is the lattice gauge coupling constant, W the Wilson loop in Z - T plane representing a pair of quark and antiquark, U_P a plaquette variable as the probe operator to measure the chromo-field strength at the point P , and L the Wilson line connecting the source W and the probe U_P . Here L is necessary to guarantee the gauge invariance of the correlator ρ_W and hence the probe is identified with $LU_P L^\dagger$. The symbol $\langle \mathcal{O} \rangle$ denotes the average of the operator \mathcal{O} in the space and the ensemble of the configurations. In the naive continuum limit $\varepsilon \rightarrow 0$, indeed, ρ_W reduces to the field strength in the presence of the $q\bar{q}$ source: $\rho_W \xrightarrow{\varepsilon \rightarrow 0} g\varepsilon^2 \langle \mathcal{F}_{\mu\nu} \rangle_{q\bar{q}} := \frac{\langle \text{tr}(ig\varepsilon^2 L \mathcal{F}_{\mu\nu} L^\dagger W) \rangle}{\langle \text{tr}(W) \rangle} + O(\varepsilon^4)$, where we have used $U_{x,\mu} = \exp(-ig\varepsilon \mathcal{A}_\mu(x))$ and hence $U_P = \exp(-ig\varepsilon^2 \mathcal{F}_{\mu\nu})$.

We measure correlators between the plaquette U_P and the chromo-field strength of the restricted field $V_{x,\mu}$ as well as the original YM field $U_{x,\mu}$. See the left panel of Fig. 1. Here the quark and antiquark source is introduced as 8×8 Wilson loop (W) in the Z - T plane, and the probe (U_P) is set at the center of the Wilson loop and moved along the Y -direction. The left and right panel of Fig. 2 show respectively the results of measurements for the chromoelectric and chromomagnetic fields $F_{\mu\nu}[U]$ for the original $SU(3)$ field U and $F_{\mu\nu}[V]$ for the restricted field V , where the field strength $F_{\mu\nu}[V]$ is obtained by using $V_{x,\mu}$ in eq(2.6) instead of $U_{x,\mu}$:

$$F_{\mu\nu}[V] := \sqrt{\frac{\beta}{6}} \rho_W[V], \quad \rho_W[V] := \frac{\langle \text{tr}(L[V] V_P L^\dagger[V] W[V]) \rangle}{\langle \text{tr}(W[V]) \rangle} - \frac{1}{3} \frac{\langle \text{tr}(V_P) \text{tr}(W[V]) \rangle}{\langle \text{tr}(W[V]) \rangle}. \quad (2.7)$$

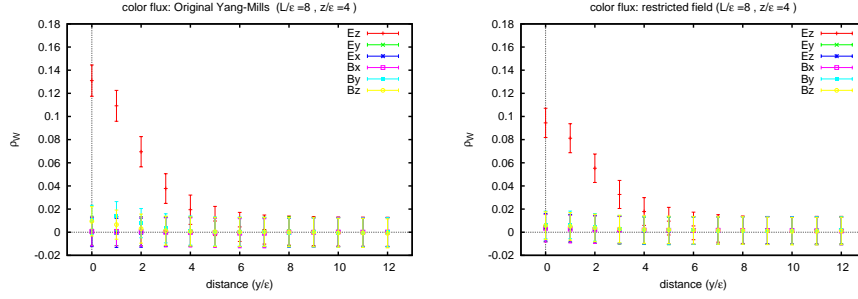


Figure 2: Measurement of components of the chromoelectric field \mathbf{E} and chromomagnetic field \mathbf{B} as functions of the distance y from the z axis. (Left panel) the original $SU(3)$ YM field, (Right panel) the restricted field.

We have checked that even if $W[U]$ is replaced by $W[V]$, together with replacement of the probe $LU_P L^\dagger$ by the corresponding V version, the change in the magnitude of the field strength $F_{\mu\nu}$ remains within at most a few percent.

3. Measurement of chromo flux on a lattice

We generate configurations of the YM gauge link variable $\{U_{x,\mu}\}$ using the standard Wilson gauge action on $L^3 \times N_T$ lattice at β : $L = 24$, $N_T = 6, 8, 10, 14, 24$ with $\beta = 6.0$; $L = 24$, $N_T = 4, 6, 8, 10, 12, 14, 24$ with $\beta = 6.2$, and $L = 24$, $N_T = 4, 6$ with $\beta = 6.4$. The gauge link decomposition $U_{x,\mu} = X_{x,\mu} V_{x,\mu}$ is obtained by the formula given in the previous section: the color field configuration $\{h_x\}$ is obtained by solving the reduction condition of minimizing the functional eq.(2.5) for each gauge configuration $\{U_{x,\mu}\}$, and then the decomposed variables $\{V_{x,\mu}\}$, $\{X_{x,\mu}\}$ are obtained by using the formula eq.(2.3). In the measurement of the Polyakov loop and Wilson loop, we apply the APE smearing technique to reduce noises [31].

3.1 Non-Abelian dual Meissner effect at zero temperature

3.1.1 Chromo flux tube

From Fig.2 we find that only the E_z component of the chromoelectric field $(E_x, E_y, E_z) = (F_{10}, F_{20}, F_{30})$ connecting q and \bar{q} has non-zero value for both the restricted field V and the original YM field U . The other components are zero consistently within the numerical errors. This means that the chromomagnetic field $(B_x, B_y, B_z) = (F_{23}, F_{31}, F_{12})$ connecting q and \bar{q} does not exist and that the chromoelectric field is parallel to the z axis on which quark and antiquark are located. The magnitude E_z quickly decreases in the distance y away from the Wilson loop.

To see the profile of the nonvanishing component E_z of the chromoelectric field in detail, we explore the distribution of chromoelectric field on the 2-dimensional plane. Fig. 3 shows the distribution of E_z component of the chromoelectric field, where the quark-antiquark source represented as 9×11 Wilson loop W is placed at $(Y, Z) = (0, 0), (0, 9)$, and the probe U is displaced on the Y - Z plane at the midpoint of the T -direction. The position of a quark and an antiquark is marked by the solid (blue) box. The magnitude of E_z is shown by the height of the 3D plot and also the contour plot in the bottom plane. The left panel of Fig. 3 shows the plot of E_z for the $SU(3)$ YM field U , and the right panel of Fig. 3 for the restricted-field V . We find that the magnitude E_z is quite uniform for the restricted part V , while it is almost uniform for the original part U except for the neighborhoods of the locations of q, \bar{q} source. This difference is due to the contributions from the remaining part X which affects only the short distance.[23]

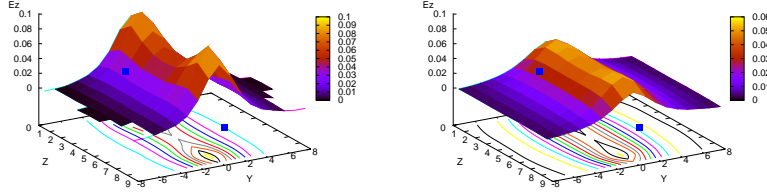


Figure 3: The distribution in Y - Z plane of the chromoelectric field E_z connecting a pair of quark and antiquark: (Left panel) chromoelectric field produced from the original YM field, (Right panel) chromoelectric field produced from the restricted $U(2)$ field.

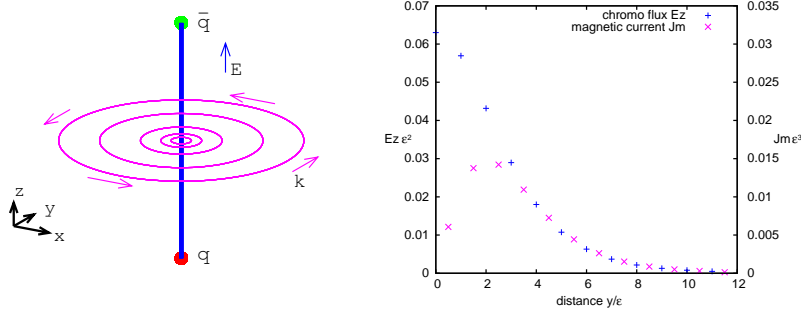


Figure 4: The magnetic-monopole current \mathbf{k} induced around the flux along the z axis connecting a quark-antiquark pair. (Left panel) The positional relationship between the chromoelectric field E_z and the magnetic current \mathbf{k} . (Right panel) The magnitude of the chromo-electronic current E_z and the magnetic current $J_m = |\mathbf{k}|$ as functions of the distance y from the z axis.

3.1.2 Magnetic current

Next, we investigate the relation between the chromoelectric flux and the magnetic current. The magnetic(-monopole) current can be calculated as

$$\mathbf{k} = *dF[\mathbf{V}], \quad (3.1)$$

where $F[\mathbf{V}]$ is the field strength (2-form) of the restricted field (1-form) \mathbf{V} , d the exterior derivative and $*$ denotes the Hodge dual operation. Note that non-zero magnetic current follows from violation of the Bianchi identity (If the field strength was given by the exterior derivative of \mathbf{V} field (one-form), $F[\mathbf{V}] = d\mathbf{V}$, we would obtain $\mathbf{k} = *d^2\mathbf{V} = 0$).

Fig. 4 shows the magnetic current measured in X - Y plane at the midpoint of quark and antiquark pair in the Z -direction. The left panel of Fig. 4 shows the positional relationship between chromoelectric flux and magnetic current. The right panel of Fig. 4 shows the magnitude of the chromoelectric field E_z (left scale) and the magnetic current k (right scale). The existence of nonvanishing magnetic current k around the chromoelectric field E_z supports the dual picture of the ordinary superconductor exhibiting the electric current J around the magnetic field B .

In our formulation, it is possible to define a gauge-invariant magnetic-monopole current k_μ by using V -field, which is obtained from the field strength $\mathcal{F}_{\mu\nu}[\mathbf{V}]$ of the field \mathbf{V} , as suggested from the non-Abelian Stokes theorem [25, 26]. It should be also noticed that this magnetic-monopole current is a non-Abelian magnetic monopole extracted from the V field, which corresponds to the stability group $\tilde{H} = U(2)$. The magnetic-monopole current k_μ defined in this way can be used to study the magnetic current around the chromoelectric flux tube, instead of the above definition of k , Eq.(3.1).

3.1.3 Type of dual superconductivity

Moreover, we investigate the type of the QCD vacuum as the dual superconductor. The left panel of Fig.5 is the plot for the chromoelectric field E_z as a function of the distance y in units of the lattice spacing ε for the original $SU(3)$ field and for the restricted field.

In order to examine the type of the dual superconductivity, we apply the formula for the magnetic field derived by Clem [33] in the ordinary superconductor based on the Ginzburg-Landau (GL) theory to the chromoelectric field in the dual superconductor. In the GL theory, the gauge field A and the scalar field ϕ obey simultaneously the GL equation and the Ampere equation:

$$(\partial^\mu - iqA^\mu)(\partial_\mu - iqA_\mu)\phi + \lambda(\phi^*\phi - \eta^2) = 0, \quad (3.2a)$$

$$\partial^\nu F_{\mu\nu} + iq[\phi^*(\partial_\mu\phi - iqA_\mu\phi) - (\partial_\mu\phi - iqA_\mu\phi)^*\phi] = 0. \quad (3.2b)$$

Usually, in the dual superconductor of the type II, it is justified to use the asymptotic form $K_0(y/\lambda)$ to fit the chromoelectric field in the large y region (as the solution of the Ampere equation in the dual GL theory). However, it is clear that this solution cannot be applied to the small y region, as is easily seen from the fact that $K_0(y/\lambda) \rightarrow \infty$ as $y \rightarrow 0$. In order to see the difference between type I and type II, it is crucial to see the relatively small y region. Therefore, such a simple form cannot be used to detect the type I dual superconductor. However, this important aspect was ignored in the preceding studies except for a work [35].

On the other hand, Clem [33] does not obtain the analytical solution of the GL equation explicitly and use an approximated form for the scalar field ϕ (given below in (3.4)). This form is used to solve the Ampere equation exactly to obtain the analytical form for the gauge field A_μ and the resulting magnetic field B . This method does not change the behavior of the gauge field in the long distance, but it gives a finite value for the gauge field even at the origin. Therefore, we can obtain the formula which is valid for any distance (core radius) y from the axis connecting q and \bar{q} : the profile of chromoelectric field in the dual superconductor is obtained:

$$E_z(y) = \frac{\Phi}{2\pi} \frac{1}{\zeta\lambda} \frac{K_0(R/\lambda)}{K_1(\zeta/\lambda)}, \quad R = \sqrt{y^2 + \zeta^2}, \quad (3.3)$$

provided that the scalar field is given by (See the right panel of Fig.5)

$$\phi(y) = \frac{\Phi}{2\pi} \frac{1}{\sqrt{2}\lambda} \frac{y}{\sqrt{y^2 + \zeta^2}}, \quad (3.4)$$

where K_ν is the modified Bessel function of the ν -th order, λ the parameter corresponding to the London penetration length, ζ a variational parameter for the core radius, and Φ external electric flux. In the dual superconductor, we define the GL parameter κ as the ratio of the London penetration length λ and the coherence length ξ which measures the coherence of the magnetic monopole condensate (the dual version of the Cooper pair condensate): $\kappa = \lambda/\xi$. It is given by [33]

$$\kappa = \frac{\lambda}{\xi} = \sqrt{2} \frac{\lambda}{\zeta} \sqrt{1 - K_0^2(\zeta/\lambda)/K_1^2(\zeta/\lambda)}. \quad (3.5)$$

According to the formula Eq.(3.3), we estimate the GL parameter κ for the dual superconductor of $SU(3)$ YM theory, although this formula is obtained for the ordinary superconductor of $U(1)$ gauge field. Table 1 shows the fitting result, and the left panel of Figure 5 shows the obtained fitted functions for YM-field and the restricted field. The superconductor is type I if $\kappa < \kappa_c$, while type II if $\kappa > \kappa_c$, where the critical value of GL parameter dividing the type of the superconductor is given by $\kappa_c = 1/\sqrt{2} \simeq 0.707$. Our data clearly shows that the dual superconductor of $SU(3)$ YM theory is type I with

$$\kappa_{YM} = 0.45 \pm 0.01. \quad (3.6)$$

	λ/ε	ζ/ε	ξ/ε	Φ	κ
SU(3) YM field	1.672 ± 0.014	3.14 ± 0.09	3.75 ± 0.12	4.36 ± 0.3	0.45 ± 0.01
restricted field	1.828 ± 0.023	3.26 ± 0.13	3.84 ± 0.19	2.96 ± 0.3	0.48 ± 0.02

Table 1: The properties of the Yang-Mills vacuum as the dual superconductor obtained by fitting the data of chromoelectric field with the prediction of the dual Ginzburg-Landau theory.

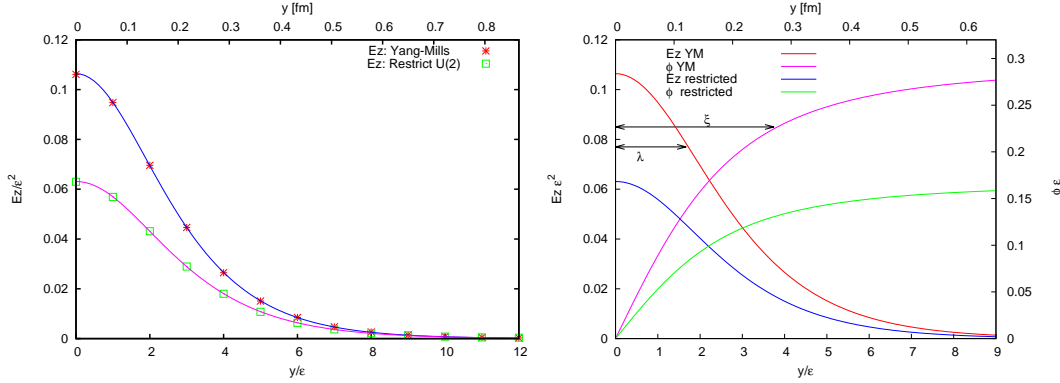


Figure 5: (Left panel) The plot of the chromoelectric field E_z versus the distance y in units of the lattice spacing ε and the fitting as a function $E_z(y)$ of y according to (3.3). The red cross for the original $SU(3)$ field and the green square symbol for the restricted field. (Right panel) The order parameter ϕ reproduced as a function $\phi(y)$ of y according to (3.4), together with the chromoelectric field $E_z(y)$.

This result is consistent with a quite recent result obtained independently by Cea, Cosmai and Papa [35]. The London penetration length $\lambda = 0.1207(17)$ fm and the coherence length $\xi = 0.2707(86)$ fm is obtained in units of the string tension $\sigma_{\text{phys}} = (440 \text{ MeV})^2$, and data of lattice spacing is taken from the TABLE I in Ref.[32]. Moreover, our result shows that the restricted part plays the dominant role in determining the type of the non-Abelian dual superconductivity of the $SU(3)$ YM theory, i.e., type I with

$$\kappa_V = 0.48 \pm 0.02, \quad (3.7)$$

$\lambda = 0.132(3)$ fm and $\xi = 0.277(14)$ fm. This is a novel feature overlooked in the preceding studies. Thus the restricted-field dominance can be seen also in the determination of the type of dual superconductivity where the discrepancy is just the normalization of the chromoelectric field at the core $y = 0$, coming from the difference of the total flux Φ . These are gauge-invariant results. Note again that this restricted-field and the non-Abelian magnetic monopole extracted from it reproduce the string tension in the static quark–antiquark potential [20, 30].

Our result should be compared with the result obtained by using the Abelian projection: Y. Matsubara et. al [34] suggests $\kappa = 0.5 \sim 1$ (which is β dependent), border of type I and type II for both $SU(2)$ and $SU(3)$. In $SU(2)$ case, on the other hand, there are other works [38, 37] which conclude that the type of vacuum is at the border of type I and type II.

3.2 Confinement/deconfinement phase transition at finite temperature

From now on, we investigate confinement/deconfinement phase transition at finite temperature in view of the dual super conductivity picture. We use Polyakov loops as quark and antiquark source in place of the Wilson loop. By measuring the chromo-flux created by the Polyakov loop pair for both the YM-field and

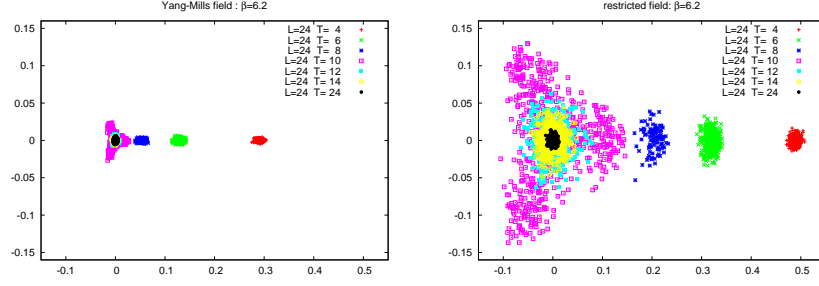


Figure 6: The distribution of the space-averaged Polyakov loop for each configuration, Eq.(3.9) (Left) For the YM field. (Right) For the restricted field.

the restricted field (V-field):

$$P_U(\vec{x}) := \text{tr} \left(\prod_{t=1}^{N_T} U(\vec{x}, t) \right), \quad P_V(x) := \text{tr} \left(\prod_{t=1}^{N_T} V(\vec{x}, t) \right), \quad (3.8)$$

we test the V-field dominance for the Polyakov loops for the various temperature. Then, we investigate the chromo-flux and the phase transition in view of the non-Abelian dual Meissner effect.

3.2.1 Polyakov loops and their correlation functions

Figure 6 show the distribution of space-averaged Polyakov loops for each configuration:

$$P_U := L^{-3} \sum_{\{\vec{x}\}} P_U(\vec{x}), \quad P_V := L^{-3} \sum_{\{\vec{x}\}} P_V(x). \quad (3.9)$$

The left panel shows the distribution of YM field and the right panel that of the V-field. We obtain the Polyakov loop average for configurations, which is the conventional order parameter for confinement and deconfinement phase transition in $SU(3)$ YM theory. Figure 7 shows the Polyakov loop average for the YM field $\langle P_U \rangle$ (left panel) and restricted field $\langle P_V \rangle$ (right panel). Each panel shows the same critical temperature of confinement/deconfinement phase transition.

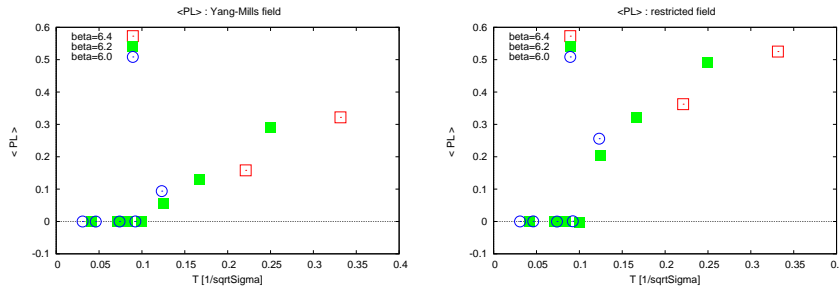


Figure 7: The Polyakov loop average: (Left) For the YM field $\langle P_U \rangle$. (Right) For the restricted field $\langle P_V \rangle$.

Then, we investigate two-point correlation function of Polyakov loop:

$$D_U(x-y) := \langle P_U(x)^* P_U(y) \rangle - \langle |P_U|^2 \rangle, \quad D_V(x-y) := \langle P_V(x)^* P_V(y) \rangle - \langle |P_V|^2 \rangle, \quad (3.10)$$

Figure 8 shows that the comparison of the $D_U(x-y)$ and $D_V(x-y)$ for each temperature. Every panel shows that the YM-field and restricted field (V-field) have the same profile, i.e., we can extract the dominant mode for the quark confinement by the V-field.

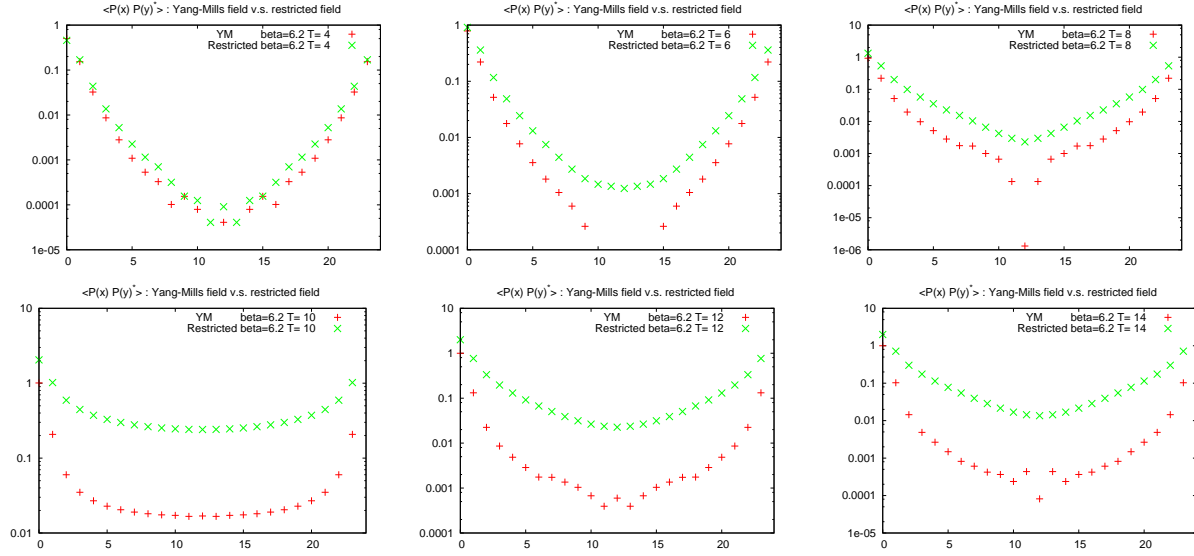


Figure 8: Comparison of the correlation function of the Polyakov loop for the YM field and the restricted field at various temperatures: The panels are arranged from the upper-left to lower-right panel in order of the high to low temperature.

3.2.2 Chromoelectric flux in deconfinement phase

Next, we investigate the non-Abelian dual Meissner effect at finite temperature. To investigate the chromo flux, we use the gauge invariant correlation function which is used at zero temperature. (see the left panel of Fig. 1). Note that at finite temperature, we must use the operator with the same size in the temporal direction, and the quark and antiquark pair is replaced by a pair of the Polyakov loop with the opposite direction.

Figure 9 shows the measurement of chromoelectric and chromomagnetic flux at high temperature $T > T_c$ (for the lattice $N_T = 6$, $\beta = 6.2$). We measure the chromo-flux of quark-antiquark pair in the plane $z = 1/3R$ for a quark at $z = 0$ and an antiquark at $z = R$ (Fig.1) by moving the probe, U_p or V_p along the y -direction. We observe the chromoelectric flux tube only in the direction connecting quark and antiquark pair, while the other components take vanishing values. We can observe no more squeezing of the chromoelectric flux tube, but non-vanishing E_y component in the chromoelectric field, which must be compared with the result at zero temperature: Fig.2. This shows the disappearance of the dual Meissner effect at high temperature.

4. Summary and outlook

We have studied the dual superconductivity for $SU(3)$ YM theory by using our new formulation of YM theory on a lattice. We have extracted the restricted field (V -field) from the YM field which plays a dominant role in confinement of quark (fermion in the fundamental representation) at finite temperature, i.e., the restricted field dominance in Polyakov loop. Then we have measured the chromoelectric and chromomagnetic flux for both the original YM field and the restricted field at low temperature in confinement phase. We have observed evidences of the dual Meissner effect of $SU(3)$ YM theory, i.e., the chromoelectric flux tube and the associated non-Abelian magnetic monopoles created by quark and antiquark pair.

At high temperature ($T > T_c$) in the deconfinement phase, we have observed the disappearance of the dual Meissner effect by measuring the chromo flux. Note that, the Polyakov loop average cannot be the di-

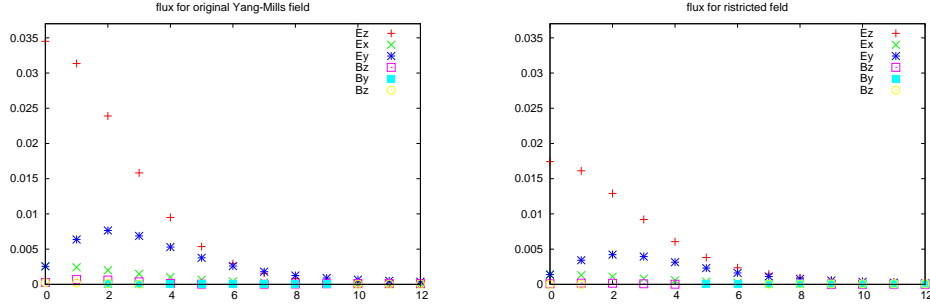


Figure 9: The chromo-flux created by quark-antiquark pair in the plane $z = 1/3R$ for a quark at $z = 0$ and an antiquark at $z = R$ (Fig.1) by moving the probe, U_p or V_p along the y-direction. (Left) For the YM-field (Right) For the restricted field.

rect signal of the dual Meissner effect or magnetic monopole condensation. Therefore, it is important to find a order parameter which detects the dual Meissner effect directly, and to investigate whether the order parameter in view of the dual Meissner effect gives the same critical temperature with that of the Polyakov loop average. At low temperature in confinement phase, we have observed non-vanishing magnetic(-monopole) current created by the quark-antiquark source, \mathbf{k} , Eq(3.1), therefore, \mathbf{k} can be the order parameter of confinement/deconfinement transition in view of dual Meissner effect. We are now under investigation on it and the result will appear in the near future.

Acknowledgement

This work is supported by Grant-in-Aid for Scientific Research (C) 24540252 from Japan Society for the Promotion Science (JSPS), and also in part by JSPS Grant-in-Aid for Scientific Research (S) 22224003. The numerical calculations are supported by the Large Scale Simulation Program No.12-13 (FY2012), No. 12/13-20 (FY2012/13) of High Energy Accelerator Research Organization (KEK).

References

- [1] Y. Nambu, Phys. Rev. D10, 4262 (1974); G. 't Hooft, in: High Energy Physics, edited by A.; Zichichi (Editorice Compositori, Bologna, 1975); S. Mandelstam, Phys. Report 23, 245 (1976); A.M. Polyakov, Nucl. Phys. B120, 429 (1977).
- [2] G. 't Hooft, Nucl. Phys. B190, 455 (1981).
- [3] T. Suzuki and I. Yotsuyanagi, Phys. Rev. D42, 4275 (1990).
- [4] J.D. Stack, S.D. Neiman and R.Wensley, Phys. Rev. D50, 3399 (1994); H. Shiba and T. Suzuki, Phys. Lett. B351 519 (1995).
- [5] J. Greensite, Prog. Part. Nucl. Phys. 51 1 (2003).
- [6] K.-I. Kondo, A.Shibata, T. Shinohara, T. Murakami, S. Kato and S. Ito, Phys. Lett. B669, 107 (2008).
- [7] A. Shibata, K.-I. Kondo and T. Shinohara, arXiv:0911.5294[hep-lat], Phys. Lett. B691, 91-98 (2010).
- [8] Y.M. Cho, Phys. Rev. D 21, 1080 (1980). Phys. Rev. D 23, 2415 (1981); Y.S. Duan and M.L. Ge, Sinica Sci. 11, 1072 (1979); L. Faddeev and A.J. Niemi, Phys. Rev. Lett. 82, 1624 (1999); S.V. Shabanov, Phys. Lett. B 458, 322 (1999). Phys. Lett. B 463, 263 (1999).
- [9] K.-I. Kondo, T. Murakami and T. Shinohara, Eur. Phys. J. C 42, 475 (2005); K.-I. Kondo, T. Murakami and T. Shinohara, Prog. Theor. Phys. 115, 201 (2006).

- [10] Y.M. Cho, Phys. Rev. Lett. 44, 1115(1980).
- [11] L. Faddeev and A.J. Niemi, Phys. Lett. B 449, 214 (1999). Phys. Lett. B 464, 90(1999).
- [12] K.-I. Kondo, T. Shinohara and T. Murakami, Prog. Theor. Phys. 120, 1 (2008).
- [13] S. Kato, K.-I. Kondo, T. Murakami, A. Shibata, T. Shinohara, and S. Ito, hep-lat/0509069, Phys. Lett. B632, 326-332 (2006).
- [14] S. Ito, S. Kato, K.-I. Kondo, A. Shibata, and T. Shinohara, Phys. Lett. B645, 67–74 (2007).
- [15] A. Shibata, S. Kato, K.-I. Kondo, T. Murakami, T. Shinohara, S. Ito, Phys.Lett. B653 101-108 (2007).
- [16] A. Shibata, S. Kato, K.-I. Kondo, T. Shinohara and S. Ito, POS(LATTICE2007) 331, arXiv:0710.3221 [hep-lat]
- [17] A. Shibata, S. Kato, K.-I. Kondo, T. Shinohara and S. Ito, 56 [hep-lat], PoS(LATTICE 2008) 268
- [18] S. Kato, K.-I. Kondo, A. Shibata and T. Shinohara, PoS(LAT2009) 228.
- [19] A. Shibata, K.-I. Kondo, S. Kato, S. Ito, T. Shinohara, N. Fukui, PoS LAT2009 (2009) 232, arXiv:0911.4533[hep-lat].
- [20] A. Shibata, K.-I. Kondo, S. Kato and T. Shinohara, PoS(Lattice 2010)286
- [21] A. Shibata, K.-I. Kondo, S. Kato and T. Shinohara, PoS LATTICE2012 (2012) 215.
- [22] A. Shibata, K.-I. Kondo, S. Kato and T. Shinohara, PoS ConfinementX (2012) 052.
- [23] A. Shibata, K.-I. Kondo, S. Kato and T. Shinohara, Phys.Rev. D87 (2013) 5, 054011, arXiv:1212.6512
- [24] K.-I. Kondo and Y. Taira, e-Print: hep-th/9911242, Prog. Theor. Phys. 104, 1189-1265 (2000). e-Print: hep-th/9906129, Mod. Phys. Lett .15, 367-377 (2000). Nucl. Phys. Proc.Suppl. 83, 497-499 (2000).
- [25] K.-I. Kondo, Phys. Rev. D77, 085029 (2008).
- [26] K.-I. Kondo and A. Shibata, arXiv:0801.4203[hep-th], CHIBA-EP-170, KEK-PREPRINT-2007-73
- [27] A. Di Giacomo, M. Maggiore, and S. Olejnik, Phys. Lett. B236, 199 (1990); Nucl. Phys. B347, 441 (1990).
- [28] Y. Matsubara, S. Ejiri and T. Suzuki, NPB Poc. suppl 34, 176 (1994)
- [29] S. Gongyo, T. Iritani and H. Suganuma, Phys. Rev. D86, 094018 (2012). H. Suganuma, K. Amemiya, H. Ichie, N. Ishii, H. Matsufuru, T. Takahashi, hep-lat/0407016, Nucl. Phys. B (Proc. Suppl.) 106, 679-681 (2002).
- [30] K.-I. Kondo, A. Shibata, T. Shinohara, and S. Kato, Phys. Rev. D83, 114016 (2011).
- [31] M. Albanese et al. (APE Collaboration), Phys. Lett. B 192,163 (1987).
- [32] R.G. Edwards, U.M. Heller and T.R. Klassen, Phys. Rev. Lett. 80, 3448–3451 (1998).
- [33] J.R. Clem, J. Low. Temp. Phys. 18, 427 (1975).
- [34] Y. Matsubara, S. Ejiri and T. Suzuki, Nucl. Phys. Proc. Suppl. 34, 176 (1994) [hep-lat/9311061].
- [35] P. Cea, L. Cosmai and A. Papa, Phys. Rev. D 86, 054501 (2012) [arXiv:1208.1362 [hep-lat]].
- [36] T. Suzuki, K. Ishiguro, Y. Mori and T. Sekido, Phys. Rev. Lett. 94, 132001 (2005) [hep-lat/0410001].
- [37] M. N. Chernodub, K. Ishiguro, Y. Mori, Y. Nakamura, M. I. Polikarpov, T. Sekido, T. Suzuki and V. I. Zakharov, Phys. Rev. D72, 074505 (2005), hep-lat/0508004.
- [38] T. Suzuki, M. Hasegawa, K. Ishiguro, Y. Koma and T. Sekido, Phys.Rev. D80, 054504(2009) arXiv:0907.0583 [hep-lat]; K. Ishiguro, M. Hasegawa, Y. Koma, T. Sekido and T. Suzuki, PoS LAT 2009, 238 (2009).